Arch Microbiol (2000) 174 : 181–188
Digital Object Identifier (DOI) 10.1007/s002030000194

ORIGINAL PAPER

J. Marquardt · E. Mörschel · E. Rhiel
M. Westermann

Ultrastructure of *Acaryochloris marina*, an oxyphotobacterium containing mainly chlorophyll *d*

Received: 2 February 2000 / Revised: 8 June 2000 / Accepted: 28 June 2000 / Published online: 2 August 2000

Abstract We present a detailed investigation of the ultrastructure of the chlorophyll *a/d*-containing unicellular oxyphotobacterium *Acaryochloris marina*, combining light and transmission electron microscopy and showing freeze fractures of this organism for the first time. The cells were 1.8–2.1 μm×1.5–1.7 μm in size. The cell envelope consisted of a peptidoglycan layer of approximately 10 nm thickness combined with an outer membrane. Cell division was intermediate between the constrictive and the septum type. The nucleoplasm, which contained several carboxysomes, was surrounded by 7–11 concentrically arranged thylakoids, which were predominantly stacked, with the exception of distinct areas where phycobiliproteins were located. The thylakoids were perforated by channel-like structures connecting the central and peripheral portions of the cytoplasm and not yet observed in other organisms. In freeze fractures, the protoplasmic fracture faces of thylakoid membranes were densely covered with particles of inhomogenous size. The particle size histogram peaked at 10–11, 13 and 18 nm. The 18-nm particles are assumed to represent photosystem I trimers. The particles on exoplasmic fracture faces, proposed to represent photosystem II complexes, were significantly larger than the corresponding particles of cyanobacteria and clustered to form large aggregates. This kind of arrangement is unique among photosynthetic organisms.

J. Marquardt (✉) · E. Rhiel
ICBM/Geomikrobiologie,
Carl von Ossietzky Universität Oldenburg,
Carl-von-Ossietzky-Strasse, 26111 Oldenburg, Germany
e-mail: juergen@africa.geomic.uni-oldenburg.de,
Fax: +49-441-7983389

E. Mörschel
Fachbereich Biologie/Zellbiologie und Angewandte Botanik,
Philipps-Universität Marburg,
Karl-von-Frisch-Strasse, 35032 Marburg, Germany

M. Westermann
Institut für Ultrastrukturforschung,
Klinikum der Friedrich-Schiller-Universität Jena,
Ziegelmühlenweg 1, 07743 Jena, Germany

Key words *Acaryochloris marina* · Carboxysomes · Cell envelope · Cyanobacteria · Freeze fractures · Oxyphotobacteria · Photosystems · Phycobiliproteins · Prochlorophytes · Thylakoid membranes

Introduction

Oxyphotobacteria contain two photosystems and are capable of performing oxygenic photosynthesis, similar to eukaryotic algae and higher plants. Usually these bacteria contain chlorophyll (Chl) *a* as the only type of chlorophyll and large phycobiliprotein aggregates (phycobilisomes) as antenna complexes and are classified as cyanobacteria. A few oxyphotobacteria, however, contain Chl *a* and Chl *b*, but no phycobilisomes. Due to their similarity to green plant chloroplasts, these bacteria were termed prochlorophytes, but later analyses revealed that they form a polyphyletic group within the cyanobacterial radiation and are more closely related to cyanobacteria than to chloroplasts (Seewaldt and Stakebrandt 1982; Palenik and Haselkorn 1992; Urbach et al. 1992).

Some years ago, another prokaryote containing two photosystems and capable of performing oxygenic photosynthesis was discovered as a symbiont of ascidians of the tropical Pacific Ocean (Miyashita et al. 1996). The bacterium was called *Acaryochloris marina*. As shown by nuclear magnetic resonance spectroscopy and fast atom bombardment mass spectroscopy, *A. marina* contains Chl *d* as a major pigment (Miyashita et al. 1997). Chl *d* differs from Chl *a* in having a formyl instead of a vinyl group at position 3 (Holt and Morley 1959). This structural change causes a red-shift of the long-wavelength absorption maximum of the pigment of about 30 nm. *A. marina* shares its host organism with the Chl *a/b*-containing bacterium *Prochloron didemni*. Thus the possession of Chl *d* might be favorable since it enables *A. marina* to utilize light that is not absorbed by *P. didemni*.

A. marina is the only organism known so far that unequivocally contains Chl *d* in vivo. It has been shown by laser flash-induced absorption changes that Chl *d* is even

present in the reaction center of photosystem I (PSI) (Hu et al. 1998a). Additionally, *A. marina* contains small amounts of Chl *a*, a Chl-*c*-type pigment, zeaxanthin, α-carotene (Miyashita et al. 1997) and at least two types of biliproteins, one of them similar to cyanobacterial phycocyanin (Hu et al. 1999). In contrast to cyanobacteria, however, the biliproteins are not organized as phycobilisomes, but as rod-shaped structures (Marquardt et al. 1997) that are attached to the cytoplasmic side of photosystem II (PSII) (Hu et al. 1999). The existence of two photosystems and the ability to perform oxygenic photosynthesis indicate that *A. marina* must be related to cyanobacteria. Its exact taxonomic position, however, is still uncertain.

With this communication we present a thorough electron microscopic examination of this organism. We combined transmission electron microscopy using different methods of cell fixation with freeze fracture studies to obtain insight into the cellular structure of *A. marina*, especially regarding the architecture of its photosynthetic apparatus.

Materials and methods

Culture conditions

Acaryochloris marina was a kind gift of Prof. S. Miyachi (Marine Biotechnology Institute, Kamaishi, Japan). The cells were grown at 20 °C in glass tubes containing 200 ml artificial sea water medium according to Jones et al. (1963). The cultures were bubbled with air enriched with 1% (v/v) CO_2 and illuminated with white fluorescent lamps, giving an electron flux density of 35 µmol photons m^{-2} s^{-1} at a light/dark regime of 16 h:8 h. Alternatively, cells were grown at ambient temperature and ambient light conditions in air-bubbled glass tubes containing Jones' medium enriched with 2.5 mM $NaHCO_3$ as carbon source. The different cultivation conditions did not cause any detectable differences in ultrastructure.

Transmission electron microscopy

For transmission electron microscopy, *A. marina* cells were washed four times in 0.1 M sodium cacodylate buffer, pH 7.2, and pre-fixed for 4 h with 4% (v/v) glutaraldehyde in cacodylate buffer. After six washes in buffer, the pre-fixed cells were post-fixed with 2% (w/v) OsO_4 in cacodylate buffer for 2.5 h, dehydrated in a graded ethanol series and embedded in Epon 812 (Serva, Heidelberg, Germany). Alternatively, cells were fixed by freeze substitution in a Bal-Tec FSU 010 freeze substitution unit (Balzers, Liechtenstein). The cells were cryofixed in liquid propane cooled by liquid nitrogen. Water exchange and fixative filtration were performed in methanol containing 1% (w/v) OsO_4, 3% (v/v) glutaraldehyde, 0.5% (w/v) uranyl acetate and 3% (v/v) H_2O for 8 h at –90 °C, followed by two 8-h periods at –60 °C and –30 °C. Cells were washed in pre-cooled acetone and incubated for 3×2 h in increasing concentrations (30%, 70%, 100%, v/v) of pre-cooled Lowicryl K4M (Lowi, Waldkraiburg, Germany) followed by UV polymerization at –30 °C overnight. Ultrathin sections were cut with an Ultracut E microtome (Reichert-Jung, Vienna, Austria) and contrasted with uranyl acetate and lead citrate (Reynolds 1963).

For immunogold labeling, the cells were fixed with 1% glutaraldehyde in culture medium for 1 h, dehydrated and cooled to –35 °C in increasing concentrations of ethanol (30–96%, v/v). The samples were then embedded in Lowicryl K4M at –35 °C overnight, followed by UV polymerization at –30 °C for 24 h. Ultrathin sections were incubated for 30 min in 10 mM Na/K-phosphate buffer (pH 7.4), 150 mM NaCl (saline phosphate buffer) containing 5% (w/v) bovine serum albumin and for 1 h in a 1:1000 dilution of an antiserum against higher-plant ribulose bisphosphate carboxylase in saline phosphate buffer with 1% (w/v) bovine serum albumin. The antiserum was a kind gift of Prof. K. Zetsche (Giessen, Germany). After ten washes in saline phosphate buffer containing 0.2% (v/v) Triton X-100 and one wash in saline phosphate buffer with 1% (w/v) bovine serum albumin, the samples were incubated with gold-coupled goat anti-rabbit IgG immunogold conjugates (British Biocell, Cardiff, UK) for 1 h to detect binding sites of the primary antibody. The size of the gold particles was 10 nm. The labeled ultrathin sections were washed ten times in saline phosphate buffer with 0.2% (v/v) Triton X-100, once in saline phosphate buffer and four times in double-distilled water. The immunogold-labeled samples were stained with uranyl acetate. Electron microscopy was performed with an EM 109 or an EM 902A transmission electron microscope (Zeiss, Oberkochen, Germany) operating at 50 or 100 kV.

Freeze fracture technique

Cells (1 ml cell suspension) were fixed with 2% (v/v) glutaraldehyde in 75 mM NaCl, 12.5 mM NaH_2PO_4, 67 mM Na_2HPO_4, pH 7.2, (phosphate-buffered saline solution) for 1 h at room temperature. Cells were washed three times in phosphate-buffered saline solution and pelleted by low-speed centrifugation. The cell pellets were resuspended in 100 µl phosphate-buffered saline solution containing 20% (w/v) glycerol as cryoprotectant and impregnated for 30 min. Small amounts of the cell suspension were enclosed between two 0.1-mm copper profiles, as used for the sandwich double-replica technique. Samples were rapidly frozen by plunging the sandwich into liquid propane cooled by liquid nitrogen. Freeze fracturing was performed in a BAF400T (Balzers, Liechtenstein) freeze fracture unit at –150 °C using a double-replica stage. The fractured samples were shadowed without etching with 2–2.5 nm Pt/C at an angle of 35°. The evaporation of Pt/C with electron guns was controlled with a thin-layer quartz crystal monitor. The replicas were cleaned with commercial sodium hypochlorite (12% w/v Cl, diluted 1:2 with distilled water), rinsed in distilled water and mounted onto uncoated copper grids for examination in a Zeiss EM 902 or EM 109 electron microscope.

Particle sizes and frequencies were determined on micrographs enlarged 100,000-fold. Sizes were measured perpendicular to the direction of shading using a magnification glass with a measuring scale with a 0.1 mm calibration. Frequencies were determined by counting the number of particles in areas of 10,000 nm^2. Means of 12 countings±standard deviation are given.

Light microscopy

Light microscopy was performed with a Zeiss Axioplan photomicroscope (Zeiss, Göttingen, Germany) equipped with an epifluorescence illuminator. DNA was visualized in cells treated with 0.5 µg 4,6-diamino 2-phenylindol dihydrochloride (DAPI) ml^{-1} by a blue fluorescence upon excitation with UV light (365 nm). Chl was excited with violet light (395–425 nm), phycobiliproteins with green light (510–560 nm).

Results and discussion

Cell envelope and division

In ultrathin sections *A. marina* cells appeared spherical to oblong with a long axis of 1.8–2.1 µm and a short axis of 1.5–1.7 µm (Fig. 1A). Cyanobacteria are very variable in size, from less than 1 µm to more than 100 µm (Castenholz and Waterbury 1989), and *A. marina* was well within

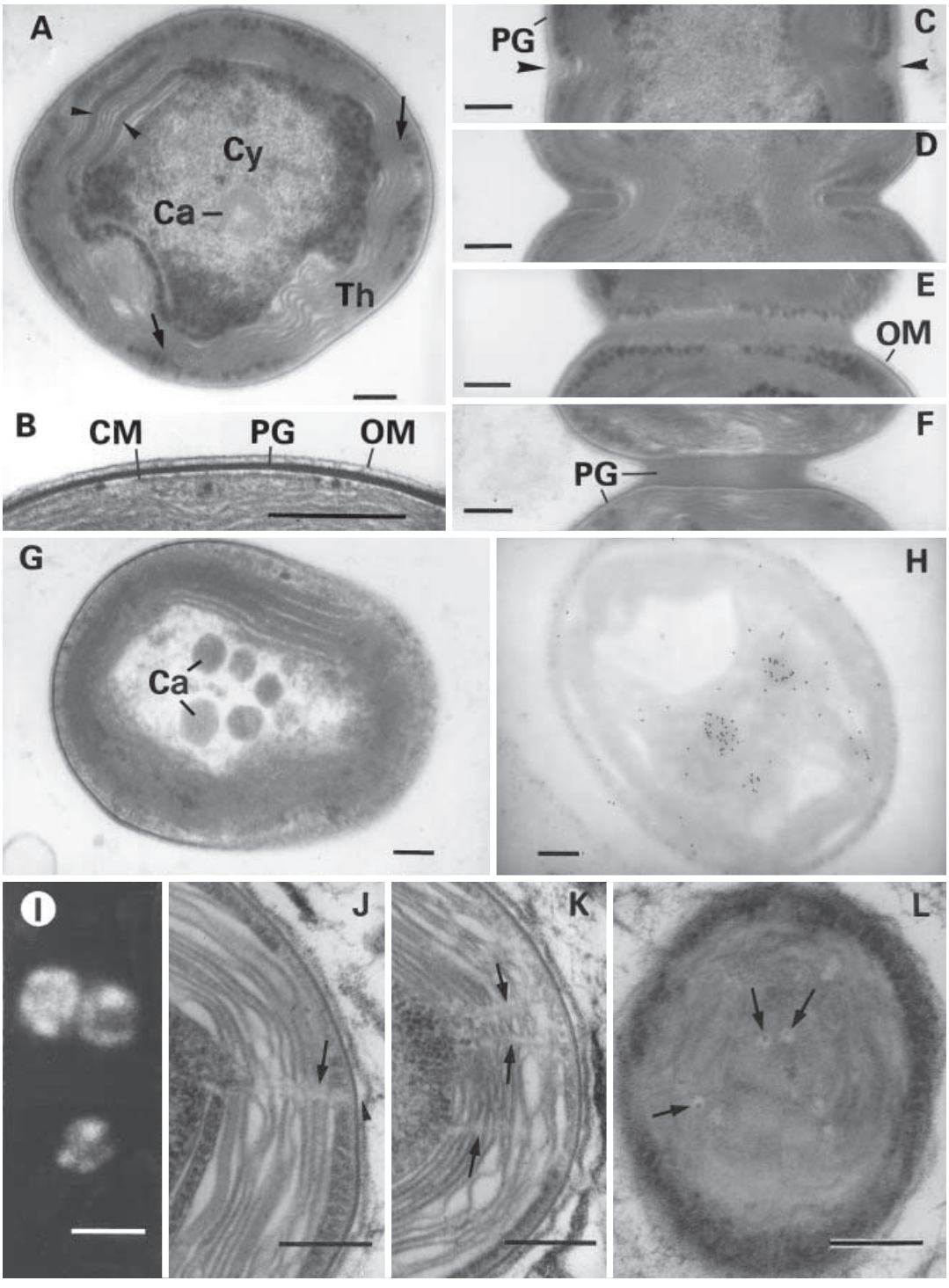

Fig. 1 **A** Electron micrograph of an ultrathin section of *Acaryochloris marina*. The central cytoplasm (*Cy*) is surrounded by several concentrically arranged thylakoids (*Th*). In the center of the cell a carboxysome (*Ca*) is visible. *Arrows* indicate channel-like structures perforating the thylakoids, *arrowheads* mark sites of biliproteins. **B** Detail of the cell envelope at higher magnification, showing outer membrane (*OM*), electron dense peptidoglycan layer (*PG*), and cytoplasmic membrane (*CM*). **C–F** Details of cells showing consecutive stages of division; *arrowheads* indicate the initial local thickening of the peptidoglycan layer. **G** Ultrathin section of a damaged cell that has lost its cytoplasm, with several carboxysomes visible. **H** Ultrathin section, immunogold-labeled with an antibody against ribulose bisphosphate carboxylase. Black dots caused by gold particles (10 nm diameter) indicate the site of the enzyme. **I** Micrograph of autofluorescent cells excited with green light (510–560 nm), showing a distinct spot-like distribution of biliproteins. **J–K** Electron micographs showing details of the thylakoid region with channel-like structures (*arrows*) and a rod-shaped structure at the cell surface (*arrowhead*). **L** Ultrathin section of a cell cut parallel to a thylakoid membrane plane, showing pores with electron-dense inclusions (*arrows*). Cells shown in **A–H** were fixed chemically, cells in **J–L** by freeze substitution. *Bars* 0.2 μm (**A–H**, **J–L**) or 2 μm (**I**)

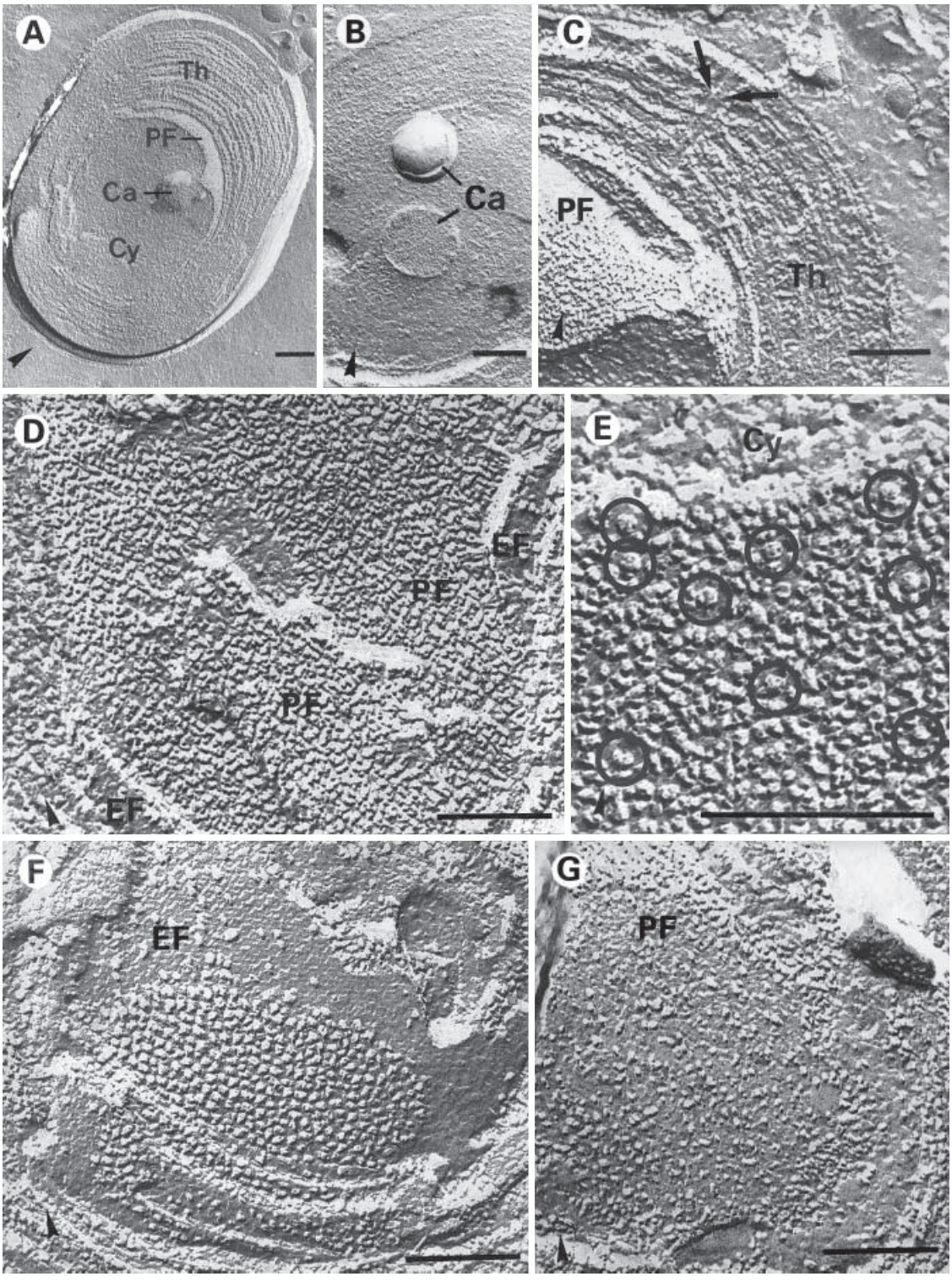

Fig. 2A–G Freeze fracture replicas of *Acaryochloris marina*. **A** Cross-fractured cell. The central cytoplasm (*Cy*), hosting a carboxysome (*Ca*) and surrounded by concentrically arranged thylakoids (*Th*), is in immediate vicinity to a periplasmic fracture face (*PF*). **B** Detail of the central cytoplasmic portion with two carboxysomes. The *lower* one is cross-fractured, the *upper* one is fractured along its surface with the shell partially splintered off. **C** Detail of thylakoids broken perpendicular to the membrane planes with a channel-like structure (*arrows*). **D** Detail of a freeze fractured cell showing regular PF faces densely covered with randomly distributed particles of inhomogenous size. **E** PF face and neighbouring central cytoplasm in higher magnification. Putative trimeric PSI complexes are encircled. **F** Detail of a cell with exoplasmic fracture faces (*EF*). Putative PSII complexes are clustered in certain regions while other areas are nearly devoid of particles. **G** Detail of a cell with a particle-depleted PF area. At the *upper* and *right-hand* edge of this area regions with high particle density are visible. *Bars* 0.2 μm. *Arrowheads* indicate the direction of shading

this range. Compared with prochlorophytes, it was much smaller than *Prochloron didemni*, which has a diameter of up to 20 μm (Newcomb and Pugh 1975). *A. marina* was rather in the size range of *Prochlorococcus marinus*, which is 0.6–0.8×1.5–1.7 μm in size (Chisholm et al. 1992).

The cells were surrounded by an envelope (Fig. 1B) similar to that described for *Synechocystis* sp. (Westermann et al. 1994) and other cyanobacteria (Drews and Weckesser 1982). The cytoplasm was covered by an electron-dense layer, generally attributed to peptidoglycan, that was separated from the cytoplasmic membrane by a narrow electron-translucent space. With a width of approximately 10 nm, the thickness of the peptidoglycan layer was in a range typical for cyanobacteria (Drews and Weckesser 1982). The outermost part of the cell wall was constituted by an outer membrane 12–15 nm thick. Cell division occurred in a manner intermediate between the constrictive and the septum type (Drews and Weckesser 1982). Division started with invagination of the cytoplasmic membrane and local thickening of the peptidoglycan layer (Fig. 1C, arrowheads). A septum was formed (Fig. 1D), followed by constrictive invagination of the outer membrane. Constriction, however, did not occur simultaneously with septum formation but was delayed. After division, the cells remained connected by a common peptidoglycan layer of 70–130 nm thickness with a slightly less electron-dense central zone (Fig. 1E). Cell separation was caused by degradation of this layer and invagination of the outer membrane (Fig. 1F). We could not observe the beginning of a second cell division as long as the cells were not separated. Therefore the spatial arrangement of consecutive planes of cell division remained unclear.

Nucleoplasm

The central cytoplasmic portion, the nucleoplasm, contained the DNA, as verified by DAPI staining (not shown). The periphery of the nucleoplasm was filled with electron-dense granular material that was also found in the space between the thylakoids and the cytoplasmic membrane (Fig. 1A). The granules might have been made up of a storage product, probably polyglucoside (Shively 1974). The nucleoplasm contained up to six polyhedral inclusion bodies of medium electron density per cell section. The inclusion bodies were approximately 170–230 nm in diameter and were best visible in broken cells that had lost their cytoplasm (Fig. 1G). These structures could also be found in freeze fractures of cells where the cytoplasm was exposed (Fig. 2A). As can be seen in Fig. 2B, the structures were surrounded by a thin envelope of approximately 3–4 nm thickness.

Polyhedral inclusion bodies are common in photoautotrophic and chemoautotrophic prokaryotes. Usually polyhedral bodies are 90–500 nm in diameter (Shively 1974). In some cyanobacteria elongated inclusion bodies several micrometers in length have been found (Gantt and Conti 1969; Jensen 1994). The polyhedral bodies have been shown to contain ribulose bisphosphate carboxylase, and subsequently were termed carboxysomes (Shively et al. 1973, 1977). Carboxysomes are surrounded by a proteinaceous shell of a few nanometers thickness (Shively et al. 1973; Jensen 1994) that is formed predominantly by the CsoS polypeptides (English et al. 1994; Baker at al. 1999).

According to their size and structure, the polyhedral particles of *A. marina* were thought also to represent carboxysomes. To check this assumption, cells were immunogold-labeled with an antibody against ribulose bisphosphate carboxylase. As shown in Fig. 1H, the antibody labeling was clustered in certain regions of the nucleoplasm with slightly higher electron density. The size and shape of these regions corresponded to those of the polyhedral inclusion bodies. An additional sparse labeling of the cytoplasmic matrix might have been due to soluble ribulose bisphosphate carboxylase.

Photosynthetic membranes

The cell periphery was filled with 7–11 layers of concentrically arranged thylakoids, appearing as a broad wavy ribbon in ultrathin sections (Fig. 1A). Occasionally, additional single thylakoids were found in the periphery of the nucleoplasm. Most of the thylakoids were "stacked," i.e. they were very close, leaving no cytoplasmic space between them. Usually cyanobacteria contain single thylakoids clearly separated from each other, with phycobilisomes attached to the cytoplasmic surface of the membranes. The thylakoids are arranged either concentrically or randomly in the cell (Gantt and Conti 1969). In this respect *A. marina* rather resembled *Prochlorococcus marinus*, which also possesses thylakoids that are closely appressed to one another (Chisholm et al. 1992).

Sometimes stacks of a few thylakoids were separated by a gap of 30–40 nm width filled with an electron-dense substance (Fig. 1A, arrowheads). As shown earlier (Hu et al. 1999), these regions are labeled by an antibody against phycocyanin and thus are believed to be the sites where the biliprotein aggregates of *A. marina* are located as large clusters. The existence of these clusters was supported by the autofluorescence pattern of the cells (Fig. 1I). When excited with violet light, preferentially absorbed by Chl, a quickly fading red autofluorescence distributed uniformly all over the cells could be seen. The red fluorescence was probably caused by Chl *a*, since the extremely long-wavelength fluorescence maximum of Chl *d* is hardly visible. When excited with green light, predominantly absorbed by phycobiliproteins, five to eight strongly fluorescent red spots approximately 0.5–1.0 μm in diameter and obviously representing the phycobiliprotein clusters could be observed in the cell peripheries (Fig. 1I). Biliproteins are also present in *Prochlorococcus marinus* (Hess et al. 1996) and it has been shown that they act as antenna pigments (Lokstein et al. 1999) and are associated with the thylakoids (Hess et al. 1999). Their precise location within this organism, however, is still unclear.

The thylakoid stacks of *A. marina* were perforated by channel-like structures connecting nucleoplasm and cell periphery. These channels were best visible in cells fixed by freeze substitution (Fig. 1J, K) but were also detectable after chemical fixation (Fig. 1A, arrows) and even in freeze fractures (Fig. 2C). The channels seemed to contain a central rod-like structure that projected towards the cytoplasmic membrane. In sections in which the cell was cut parallel to a thylakoid surface, electron-translucent pores of about 30 nm diameter were visible in the more electron-dense membrane plane (Fig. 1L). Inside some of the pores a circular or elliptical structure of high electron density was detectable. The structure was about 12–18 nm in diameter. To our knowledge channel-like structures perforating the thylakoids have not been found in other organisms. Microtubule arrays located near the thylakoids have been found in the cyanobacterium *Cyanothece* sp. strain PCC8303 (Porta et al. 2000), but these microtubules did not penetrate the membranes.

We assume that the channels might be important for exchange processes between the central and the peripheral portion of the cytoplasm and that the rod-shaped structures might serve to stabilize them. The channels might also be a kind of intracellular extensions of sex pili, important for the export of genetic material. Pilus-like particles were frequently found in negatively contrasted culture solution (not shown), and occasionally a rod-shaped structure could be found at the cell surface in the region where the central structure of a channel projected towards the cytoplasmic membrane (Fig. 1J, arrowhead). Intracellular extensions of sex pili are not known from other prokaryotes, but pilin-like proteins have been found in thylakoids of the cyanobacterium *Synechocystis* sp. strain PCC 6803 (He and Vermaas 1999). One might also suppose that the structures represent filamentous viruses. However, their low number per cell is untypical for a viral infection, and viruses infecting cyanobacteria in general are polyhedral and not filamentous (e.g. Wilson et al. 1993).

In freeze fractures through the thylakoid region, two types of fracture faces could clearly be distinguished by their appearance. By its location in immediate vicinity to the central cytoplasmic portion of the cell, one of the fracture faces could be identified as the protoplasmic fracture face (Fig. 2A,C,E). As in cyanobacteria, in which the protoplasmic fracture face contains most of the protein complexes of the thylakoids, with the exception of PSII, it was densely covered with randomly distributed particles of a rather inhomogenous size (Fig. 2D). The particle size histogram (Fig. 3A) showed peaks at 10–11, 13 and 18 nm, with most of the particles falling into the 10–11 nm class. In *Synechocystis* sp., the highest peak in the particle size histogram of thylakoid protoplasmic fracture faces is also at 10 nm (Westermann et al. 1994). The large particles, centered around 18 nm, might be assigned to trimeric PSI complexes. The occurrence of such complexes has repeatedly been reported for oxyphotobacteria (e.g. Van der Staay et al. 1993; Westermann et al. 1999), and they have also been isolated from *A. marina* as particles 21 nm in diameter (Hu et al. 1998b). Indeed, the fracture face hosted several particles of this size class which had the typical shape of trimeric PSI (Fig. 2E, circles). The size difference between isolated particles and the presumed PSI trimers in the freeze fractures might have been due to the detergent covering of the isolated complexes. The particle frequency in the protoplasmic fracture face was 3983±581 per μm^2, similar to values found for protoplasmic fracture faces of some cyanobacteria (Westermann et al. 1994). This value, however, might vary with changing environmental conditions.

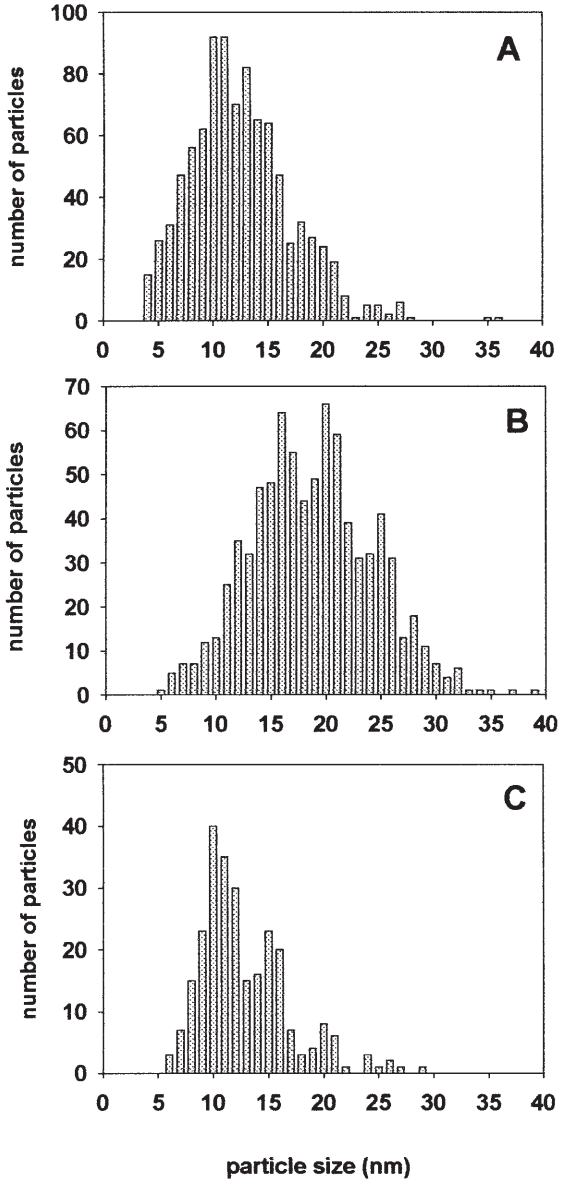

Fig. 3 Particle size histograms of regular periplasmic fracture faces (**A**), exoplasmic fracture faces (**B**) and periplasmic fracture faces with lower particle density (**C**)

The second type of fracture face in the thylakoid region is proposed to represent the exoplasmic fracture faces (Fig. 2F). In cyanobacteria this fracture face con-

tains the PSII particles, which are arranged in parallel rows (Mörschel and Schatz 1987). In *A. marina*, however, no parallel rows were detectable. Instead, the particles were concentrated in large clusters, while other regions of the fracture face were almost devoid of them. The particle density within the clusters was 2575±295 per μm^2. The particle size histogram (Fig. 3B) showed major maxima at 16 and 20 nm, with smaller maxima at 12 and 25 nm. Hence the exoplasmic fracture face particles of *A. marina* were significantly larger than in cyanobacteria, in which the particle size histograms peak at 10 and 15 nm (Westermann et al. 1994), corresponding to the 10×15 nm of dimeric PSII complexes. The larger size of PSII particles in *A. marina* might be a hint for the existence of an additional PSII antenna in this organism. Interestingly, a probe against the *fcp2* gene, which encodes for a light-harvesting polypeptide of the diatom *Cyclotella cryptica*, reacted with *A. marina* DNA, but not with the DNA from the cyanobacterium *Merismopedia* sp. (M. Hust, ICBM/Geomikrobiologie, Universität Oldenburg, Germany, personal communication). Further work on the molecular level is necessary to obtain more detailed information.

Another type of fracture face was found less frequently (Fig. 2G). It obviously formed a continuum with the periplasmic fracture faces described above, as could be seen at the edges of this fracture face type. However, the particle size histogram of this area (Fig. 3C) showed peaks at 10 and 15 nm, indicating a slightly modified protein complex composition. Additionally, and more striking, the particle density was 2000±311 per μm^2, only about half the value found for regular periplasmic fracture faces. The diameter of the particle-depleted areas corresponded to that at the assumed PSII clusters, and we suppose that this type of fracture face represented periplasmic fracture faces in the regions where PSII centers were aggregated in the exoplasmic fracture faces.

The clustering of the exoplasmic fracture face particles can also be correlated with the occurrence of phycobiliproteins in certain restricted thylakoid areas. The particle clusters were even in the size range of the red fluorescent spots found by light microscopy. The restriction of phycobiliproteins to certain membrane areas and the fact that they are exclusively bound to PSII but not to PSI (Hu et al. 1999) raised the question whether there is a spatial separation of PSII and PSI or a PSII heterogeneity with PSII centers in other membrane areas devoid of phycobiliprotein antennae (Hu et al. 1999). The results of our freeze fracture experiments solve this problem and clearly show that there was no PSII heterogeneity, but rather a lateral heterogeneity of the thylakoids with two distinct domains. One contained PSII and its phycobiliprotein antenna while the other one was enriched in PSI. A spatial separation of PSI and PSII is also found in green plants and in prochlorophytes (Van der Staay and Staehelin 1994). A separation of PSI and PSII has been suggested to be favorable for energetic reasons (Trissl and Wilhelm 1993). In plants and prochlorophytes, PSII is concentrated in the stacked membranes while PSI is enriched in the unstacked thylakoids. This is in contrast to *A. marina*, in which the membranes devoid of PSII are stacked. In green plants, the light-harvesting complexes of PSII are involved in membrane stacking (Carter and Staehelin 1980; Mullet 1983; Day et al. 1984). The mechanism for the thylakoid stacking in *A. marina* is unclear.

It can be summarized that *A. marina* shares many ultrastructural features with other oxyphotobacteria, e.g. the structure of the cell envelope, the mode of cell division and the possession of carboxysomes. However, its photosynthetic apparatus is unique among photosynthetic organisms, not only by the occurrence of Chl *d* and the organization of the phycobiliproteins, but also by the overall architecture of the photosynthetic membranes.

Acknowledgements The authors thank M. Johannsen, R. Kort, and G. Niemann for their excellent technical assistance. E.R. and J.M. are indebted to the students of their electron microscopy course, D. Morozova, J. Behrends, and K. Silberberg, for contributing some of the figures shown in this communication. The financial support of the Deutsche Forschungsgemeinschaft to E.M. and M.W. (SFB 197) is gratefully acknowledged.

References

Baker SH, Lorbach SC, Rodriguez-Buey M, Williams DS, Aldrich HC, Shively JM (1999) The correlation of the gene *csoS2* of the carboxysome operon with two polypeptides of the carboxysome in *Thiobacillus neapolitanus*. Arch Microbiol 172: 233–239

Carter DP, Staehelin LA (1980) Proteolysis of chloroplast thylakoid membranes. II. Evidence for the envolvement of the light-harvesting chlorophyll *a/b*-protein complex in thylakoid stacking and for effects of magnesium ions on photosystem II-light-harvesting complex aggregates in the absence of membrane stacking. Arch Biochem Biophys 200:374–386

Castenholz RW, Waterbury JB (1989) Oxygenic photosynthetic bacteria, group I. Cyanobacteria, preface. In: Staley JT (ed) Bergey's manual of systematic bacteriology, vol 3. Williams and Wilkins, Baltimore, pp 1710–1727

Chisholm SW, Frankel SL, Goericke R, Olson RJ, Palenik B, Waterbury JB, West-Johnsrud L, Zettler ER (1992) *Prochlorococcus marinus* nov. gen. nov. sp.: an oxyphototrophic prokaryote containing divinyl chlorophyll *a* and *b*. Arch Microbiol 157: 297–300

Day DA, Ryrie IJ, Fuad N (1984) Investigations of the role of the main light-harvesting chlorophyll-protein complex in thylakoid membranes. Reconstitution of depleted membranes from intermittent-light-grown plants with the isolated complex. J Cell Biol 98:163–172

Drews G, Weckesser J (1982) Function, structure and composition of cell walls and external layers. In: Carr NG, Whitton BA (eds) The biology of cyanobacteria. Blackwell, Oxford, pp 333–357

English RS, Lorbach SC, Qin X, Shively JM (1994) Isolation and characterization of a carboxysome shell gene from *Thiobacillus neapolitanus*. Mol Microbiol 12:647–654

Gantt E, Conti SF (1969) Ultrastructure of blue-green algae. J Bacteriol 97:1486–1493

He Q, Vermaas W (1999) Genetic deletion of proteins resembling Type IV pilins in *Synechocystis* sp. PCC 6803: their role in binding or transfer of newly synthesized chlorophyll. Plant Mol Biol 39:1175–88

Hess WR, Partensky F, van der Staay GWM, Garcia-Fernandez JM, Börner T, Vaulot D (1996) Coexistence of phycoerythrin and a chlorophyll *a/b* antenna in a marine prokaryote. Proc Natl Acad Sci 93:11126–11130.

Hess WR, Steglich C, Lichtlé C, Partensky F (1999) Phycoerythrins of the oxyphotobacterium *Prochlorococcus marinus* are associated to the thylakoid membrane and are encoded by a single large gene cluster. Plant Mol Biol 40:507–521

Holt AS, Morley HV (1959) A proposed structure for chlorophyll *d*. Can J Chem 37:507–514

Hu Q, Miyashita H, Iwasaki I, Kurano N, Miyachi S, Iwaki M, and Itoh S (1998a) A photosystem I reaction center driven by chlorophyll *d* in oxygenic photosynthesis. Proc Natl Acad Sci USA 95:13319–13323

Hu Q, Ishikawa T, Inoue Y, Miyashita H, Kurano N, Miyachi S, Iwaki M, Itoh S, Marquardt J, Mörschel E (1998b) Heterogeneity of chlorophyll *d*-binding photosystem I reaction centers from the photosynthetic prokaryote *Acaryochloris marina*. In: Garab G (ed) Photosynthesis: mechanisms and effects, vol I. Kluwer, Dordrecht, pp 437–440

Hu Q, Marquardt J, Iwasaki I, Miyashita H, Kurano N, Mörschel E, Miyachi S (1999) Molecular structure, localization and function of biliproteins in the chlorophyll *a/d* containing oxygenic photosynthetic prokaryote *Acaryochloris marina*. Biochim Biophys Acta 1412:250–261

Jensen TE (1994) Fine structure of elongate polyhedral bodies (carboxysomes) in two *Oscillatoria* (Cyanophyceae) isolates. Microbios 79:203–214

Jones RF, Speer HL, Kury W (1963) Studies on the growth of the red alga *Porphyridium cruentum*. Physiol Plant 16:636–643

Lokstein H, Steglich C, Hess WR (1999) Light-harvesting antenna function of phycoerythrin in *Prochlorococcus marinus*. Biochim Biophys Acta 1410:97–98

Marquardt J, Senger H, Miyashita H, Miyachi S, Mörschel E (1997) Isolation and characterization of biliprotein aggregates from *Acaryochloris marina*, a *Prochloron*-like prokaryote containing mainly chlorophyll *d*. FEBS Lett 410:428–432

Miyashita H, Ikemoto H, Kurano N, Adachi K, Chihara M, Miyachi S (1996) Chlorophyll *d* as a major pigment. Nature 383:402

Miyashita H, Adachi K, Kurano N, Ikemoto H, Chihara M, Miyachi S (1997) Pigment composition of a novel oxygenic photosynthetic prokaryote containing chlorophyll *d* as the major chlorophyll. Plant Cell Physiol 38:74–281

Mörschel E, Schatz GH (1987) Correlation of photosystem-II complexes with exoplasmic freeze-fracture particles of thylakoids of the cyanobacterium *Synechococcus* sp. Planta 172: 145–154

Mullet JE (1983) The amino acid sequence of the polypeptide segment which regulates membrane adhesion (grana stacking) in chloroplasts. J Biol Chem 258:9941–9948

Newcomb EH, Pugh TD (1975) Blue-green algae associated with ascidians of the Great Barrier Reef. Nature 253:533–534

Palenik B, Haselkorn R (1992) Multiple evolutionary origins of prochlorophytes, the chlorophyll *b*-containing prokaryotes. Nature 355:265–267

Porta D, Rippka R, Hernández-Mariné M (2000) Unusual ultrastructural features in three strains of *Cyanothece* (cyanobacteria). Arch Microbiol 173:154–163

Reynolds ES (1963) The use of lead citrate at high pH as an electron opaque stain in electron microscopy. J Cell Biol 17: 208–212

Seewaldt E, Stackebrandt E (1982) Partial sequence of 16 S ribosomal RNA and the phylogeny of *Prochloron.* Nature 295: 618–620

Shively JM (1974) Inclusion bodies of prokaryotes. Annu Rev Microbiol 28:167–187

Shively JM, Ball FL, Kline BW (1973) Electron microscopy of the carboxysomes (polyhedral bodies) of *Thiobacillus neapolitanus*. J Bacteriol 116:1405–1411

Shively JM, Bock E, Westphal K, Cannon GC (1977) Icosahedral inclusions (carboxysomes) of *Nitrobacter agilis*. J Bacteriol 132:873–675

Trissl H-W, Wilhelm C (1993) Why do thylakoid membranes from higher plants form grana stacks? Trends Biochem Sci 18: 415–419

Urbach E, Robertson DL, Chisholm SW (1992) Multiple evolutionary origins of prochlorophytes within the cyanobacterial radiation. Nature 355:267–270

Van der Staay GWM, Staehelin LA (1994) Biochemical characterization of protein composition and protein phosphorylation patterns in stacked and unstacked thylakoid membranes of the prochlorophyte *Prochlorothrix hollandica.* J Biol Chem 269: 24834–24844

Van der Staay GWM, Boekema EJ, Dekker JP, Matthijs HCP (1993) Characterization of trimeric photosystem I particles from the prochlorophyte *Prochlorothrix hollandica* by electron microscopy and image analysis. Biochim Biophys Acta 1142: 189–193

Westermann M, Ernst A, Brass S, Böger P, Wehrmeyer W (1994) Ultrastructure of cell wall and photosynthetic apparatus of the phycobilisome-less *Synechocystis* sp. strain BO 8402 and the phycobilisome-containing derivative strain BO 9201. Arch Microbiol 162:222–232

Westermann M, Neuschaefer-Rube O, Mörschel E, Wehrmeyer W (1999) Trimeric photosystem I complexes exist in vivo in thylakoid membranes of the *Synechocystis* strain BO 9201 and differ in absorption characteristics from monomeric photosystem I complexes. J Plant Physiol 155:24–33

Wilson WH, Joint IR, Carr NG, Mann NH (1993) Isolation and molecular characterization of five marine cyanophages propagated on *Synechococcus* sp. strain WH7803. Appl Environ Microbiol 59:3736–3743